# The physical oceanography of the Bering Sea: A summary of physical, chemical, and biological characteristics, and a synopsis of research on the Bering Sea

**Phyllis J. Stabeno,[1] James D. Schumacher,[1] and Kiyotaka Ohtani[2]**

**[1]NOAA, Pacific Marine Environmental Laboratory, 7600 Sand Point Way NE, Seattle, Washington 98115**
**[2]Laboratory of Physical Oceanography, Hokkaido University, Hokkaido, Japan**

**in *Dynamics of the Bering Sea: A Summary of Physical, Chemical, and Biological Characteristics, and a Synopsis of Research on the Bering Sea*, T.R. Loughlin and K. Ohtani (eds.), North Pacific Marine Science Organization (PICES), University of Alaska Sea Grant, AK-SG-99-03, 1–28.**

# Introduction

The Bering Sea is a semi-enclosed, high-latitude sea that is bounded on the north and west by Russia, on the east by Alaska, and on the south by the Aleutian Islands (Fig. 1). It is divided almost equally between a deep basin (maximum depth 3,500 m) and the continental shelves (<200 m). The broad (>500 km) shelf in the east contrasts with the narrow (<100 km) shelf in the west. Seasonal extremes occur in solar radiation, meteorological forcing, and ice cover. Large interannual fluctuations exist in climate, due both to the Southern Oscillation and the Pacific-North American atmospheric pressure patterns (Niebauer 1988; Niebauer et al., chapter 2, this volume). An amplification of global warming is predicted in the Bering Sea (Bryan and Spelman 1985). Basin scale climate variability profoundly impacts both the physical and biological environment (Schumacher and Alexander, chapter 6, this volume).

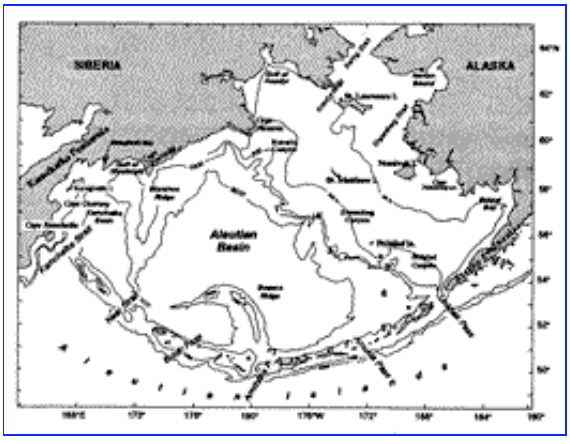


**Fig. 1. Geography and place names of the Bering Sea. The location of the seven mooring sites discussed in the text are indicated by bold numerals. Depth contours are in meters.**

Interactions among ocean, ice, and atmosphere dominate the physics of the Bering Sea. Large-scale weather patterns in both the tropical South Pacific (El Niño-Southern Oscillation events) and the North Pacific (Pacific-North America patterns) have strong connections to the Bering Sea, mainly via the atmosphere (Niebauer 1988, Niebauer and Day 1989, Niebauer et al., chapter 2, this volume). The mode of teleconnection appears to perturb the passage of storms (areas of low sea level atmospheric pressure with closed isobars) along the Aleutian Island chain. The migration of storms results in a statistical feature known as the Aleutian Low, one of the two main low pressure systems in the high latitude Northern Hemisphere. During summer with its long periods of daylight and high insolation, the Aleutian Low is typically weak and weather benign. During winter, a marked change occurs in atmospheric pressure fields. High sea level pressure (Siberian High) dominates Asia, while the Aleutian Low intensifies and dominates weather over the North Pacific and Bering Sea. The juxtaposition of these features results in strong, frigid winds from the northeast. The frequency and intensity of storms in the southern Bering Sea decreases from winter to summer and frequency also decreases with increasing latitude (Overland 1981, Overland and Pease 1982). In the winter, an average of three to five storms per month move eastward along the Aleutian Chain forming the primary storm track, while less than two storms per month cross the northern Bering Sea. A secondary storm track curves northward along the Asian coast. A difference in the number of storms also occurs across the broad shelf, with more activity occurring over the outer shelf (Schumacher and Kinder 1983).

Due to the presence of the Aleutian Low, the wind torque over the Bering Sea is greater in winter than in summer by an order of magnitude. A climatology of the wind forcing (Bond et al. 1994) shows that eastward and northward-propagating storm systems dominate the surface stress at short periods (<1 month), and their energy mixes the upper ocean. At longer periods (>1 month), the wind-driven (Sverdrup) transport accounts for roughly one-half of the observed transport in the Kamchatka Current. Driven by changes in the location of the Aleutian Low, interannual variations in the Sverdrup transports occur that are ~25% of the mean.

Much of the physical oceanographic research in the Bering Sea has been coupled to fisheries research, since the combination of nutrient-rich slope waters and high summer solar radiation create one of the world's most productive ecosystems (Walsh et al. 1989). Seasonal primary production often begins with a bloom on the shelf associated with ice-edge melt; annual production varies from >200 g C/m$^2$ over the southeastern shelf to >800 g C/m$^2$ north of St. Lawrence Island. Over the western shelf maximum annual production (>400 g C/m$^2$) occurs over the continental slope (Arzhanova et al. 1995). These blooms often consume all available nutrients (Niebauer et al. 1995), so subsequent production depends on nutrients being supplied by mixing due to storms and/or advection. The blooms support strong higher trophic level production which in turn supports vast populations of marine mammals, birds, fish, and shellfish. During the mid-1980s, the pollock fishery was the world's largest single species fishery, and during the mid-1990s the salmon run along the Alaska Peninsula was the world's largest.

This paper both reviews and presents new data on the physical oceanography of the Bering Sea. It will focus on the basin, since a thorough review of the shelves has recently been completed (Schumacher and Stabeno 1998). Further, since this volume contains an extensive review of the water property characteristics (Luchin et al., chapter 3, this volume), the primary goal here is to review and update circulation over the basin. We begin with the known and estimated transports through each of the passes of the Aleutian Islands, followed by a discussion of the surface and deep currents of the Bering Sea basin and the flow on the Bering Sea shelves.

# General Circulation

The circulation in the Bering Sea basin (Fig. 2) is often described as a cyclonic gyre, with the southward flowing Kamchatka Current forming the western boundary current and the northward flowing Bering Slope Current forming the eastern boundary current. Circulation in the Bering Sea is strongly influenced by the Alaskan Stream, which enters the Bering Sea through the many passes in the Aleutian Arc. The inflow into the Bering Sea is balanced by outflow through Kamchatka Strait, so that circulation in the Bering Sea basin may be more aptly described as a continuation of the North Pacific subarctic gyre. Circulation on the eastern Bering Sea shelf is generally northwestward. The net northward transport through the Bering Strait, while important to the Arctic Ocean, has virtually no effect on the circulation in the Bering Sea basin. It does, however, play the dominant role in determining the circulation on the northern shelf. The currents of the Bering Sea have been examined principally through inferred baroclinic flow and to a lesser extent by drifting buoys, current meter moorings, and models.

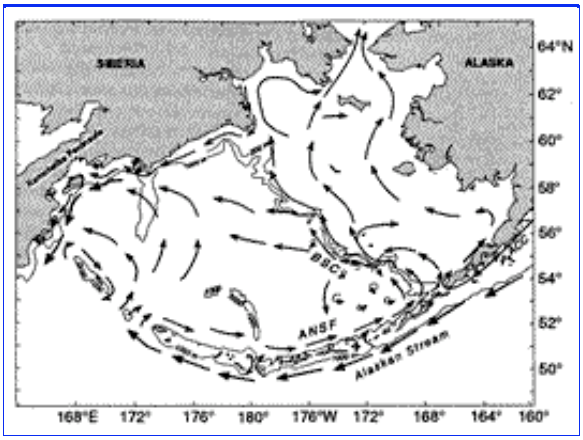


**Fig. 2. Schematic of mean circulation in the upper 40 m of water column over the basin and shelf (after Stabeno and Reed 1994, Schumacher and Stabeno 1998). The arrows with solid heads represent currents with mean speeds typically >50 cm/s. The Alaskan Stream, Kamchatka Current, Bering Slope Current, and Aleutian North Slope Current are each indicated. The triangles with numbers indicate the location of the seven deep moorings (water depth >1,000 m) discussed in the paper. The 100-m flow and 1,000-m isobath are indicated.**

## Passes

The passes play a primary role in determining both circulation and distribution of water properties. The Aleutian Arc forms a porous boundary between the Bering Sea and the North Pacific (Fig. 3). Even though only three passes (Amchitka Pass, Near Strait, and Kamchatka Strait) extend deeper than 700 m, there is significant flow through many of the 14 main passes. Transport into the Bering Sea can vary by more than a factor of two and this affects the transport in the Kamchatka Current. The strong variability of flow through the passes has time scales which vary from weeks to years. The source of most of the flow into the Bering Sea basin is the Alaskan Stream, the northern boundary of the cyclonic North Pacific subarctic gyre. It provides relatively fresh surface waters and warm subsurface water.

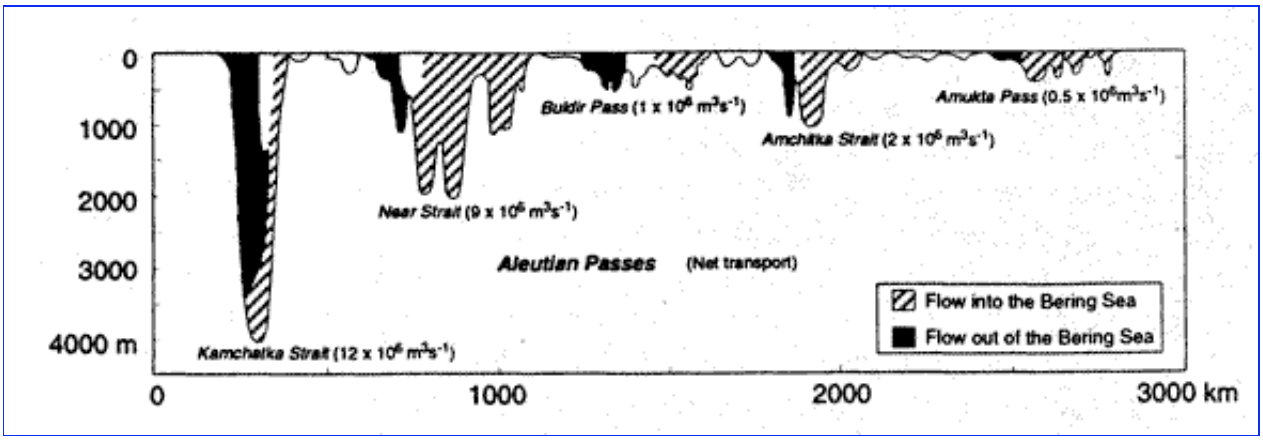


**Fig. 3. A cross section of the passes of the Aleutians. Suspected or measured transports are given for each of the main passes. The hatched regions indicate northward flow and the dotted regions indicate southward flow. Unshaded regions indicate areas where either the flow is variable or unknown.**

We first explore flow through the two passes on the eastern Bering Sea shelf, Unimak Pass (at the south), and Bering Strait (at the north). The influence of these passes is limited to the eastern Bering Sea shelf and plays virtually no role in modifying currents in the basin. We next examine flow through the major passes in the Aleutian Arc (starting on the eastern side and moving westward), which strongly influence the flow patterns and water properties of the basin.

### Shelf Passes

Unimak Pass forms the only significant conduit between the shelves of the Gulf of Alaska and the eastern Bering Sea. This relatively shallow (<80 m) and narrow (~30 km) pass permits flow of a portion of the Alaska Coastal Current (ACC) into the Bering Sea. The ACC extends 1000 km along the Gulf of Alaska coast from southern Alaska to Unimak Pass (Stabeno et al. 1995). A recent study of flow through Unimak Pass (Reed and Stabeno, submitted) substantiates the earlier conjecture (Schumacher et al. 1982) that a strong seasonal signal in transport exists. The current appears to be uniform across the pass. Transport is predominantly baroclinic (>70%). Net baroclinic transport is northward with a maximum in the fall and winter (>0.50 × $10^6$ $m^3/s$), a minimum in the late spring and summer (~0.10 × $10^6$ $m^3/s$), and a mean transport of 0.23 × $10^6$ $m^3/s$. Maximum daily-averaged barotropic flow is also northward and can exceed 100 cm/s in the winter (tidal currents can strengthen this, resulting in the flow exceeding 200 cm/s), although it is weak during the summer. The barotropic flow through this pass results from sea level changes induced by winds along the peninsula (Schumacher et al. 1982). While direct observations do not exist to establish the magnitude of the long-term variability, the portion of transport resulting from winds likely varies significantly.

Of all the passes that connect the surrounding oceans with the Bering Sea, only the physical oceanography of Bering Strait is well documented (Coachman et al. 1975, Aagaard et al. 1985a, Roach et al. 1995). An approximate 0.4 m mean sea level difference between the Bering Sea and Arctic Ocean drives a net northward transport (~0.8 × $10^6$ $m^3/s$) through Bering Strait (Coachman 1993). Reversals of the northward flow occur during periods of southward winds. The strongest winds occur during the autumn/winter, resulting in a seasonal signal in the transport. The strongest monthly mean northward transport through Bering Strait occurs in July (~1.4 × $10^6$ $m^3/s$), and the weakest in December (0.3 × $10^6$ $m^3/s$). Thus the annual signal is out of phase with the inflow through Unimak Pass. There is also strong intra-annual variability,

with mean annual transports ranging from $0.6 \times 10^6$ m$^3$/s to $>1.0 \times 10^6$ m$^3$/s.

The northward flow through Bering Strait strongly influences the currents over much of the northern Bering Sea shelf. One consequence of the northward transport is that a supply of nutrient-rich water to the northern shelf upwells near St. Lawrence Island, thereby stimulating primary production (Nihoul et al. 1993). The northward flow also provides the only connection and exchange of water between the Pacific and Atlantic Oceans in the Northern Hemisphere. During ice formation, cold saline water (>34 psu and <–1.5°C) is produced over the northern shelf and flows northward through Bering Strait. Globally, this water plays a role both in maintaining the Arctic Ocean halocline and in ventilation of the deep waters (Aagaard et al. 1985a).

**Deep Aleutian Passes**

The easternmost major conduit between the North Pacific Ocean and the Bering Sea is Amukta Pass (Figs. 1 and 3). Recent measurements have shown that the net baroclinic transport through this pass is highly variable (Reed and Stabeno 1997), ranging from $1.4 \times 10^6$ m$^3$/s northward to a weak ($<0.10 \times 10^6$ m$^3$/s) southward flow, with a mean of $0.6 \times 10^6$ m$^3$/s. Maximum northward geostrophic speeds vary from 25 to 73 cm/s, while the southward speeds are weaker (7–32 cm/s).

This transport, along with the flow through Amchitka Pass, is the source of the Aleutian North Slope Current (Reed and Stabeno, chapter 8, this volume) and ultimately the Bering Slope Current. The width of the pass is sufficient (greater than the internal Rossby radius) that there is generally northward flow on the east side and southward flow on the west side. The relative strength of these two branches determines the direction and magnitude of the net transport. The source of the flow through this pass is usually the Alaskan Stream; however, at times (~10%) the eastward flow on the north side of the Aleutian Islands turns southward through the western side of the pass and retroflects through the eastern side. A more common scenario, however, is that the Alaskan Stream enters on the eastern side of the pass with some retroflecting, supplying a portion of the southward branch.

Two conductivity temperature depth (CTD) sections across Amukta Pass, done a year apart during August (Fig. 4), show water properties during a period of strong (Fig. 4a, b) and of weak (Fig. 4c, d) inflow. The warm water in the upper 100 m during both years resulted from summer warming. The warm water at depth during 1994 resulted from Alaskan Stream inflow, while during 1995 there was little inflow of Alaskan Stream water. While variability on time scales of days exists, the data presented in Reed (1995) and Reed and Stabeno (1997) suggest that inflow of Alaskan Stream water through Amukta Pass varies mainly on the time scale of months to years.

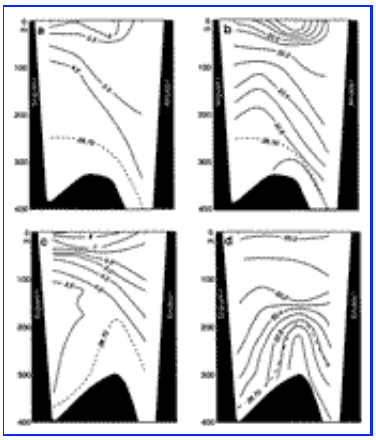

**Fig. 4. (a) Vertical sections of temperature (°C) and (b) salinity (psu) in Amukta Pass in August 23, 1994, during a period of strong inflow (net 1.0 × $10^6$ $m^3$/s) of Alaskan Stream water into the Bering Sea. (c) Vertical sections of temperature (°C) and (d) salinity (psu) during a period of weak (net flow 0.1 × $10^6$ $m^3$/s) outflow from the Bering Sea.**

In the Aleutian Basin, a subsurface temperature maximum occurs between 150 and 400 m. The sigma-*t* density of the maxima is between 26.6 and 26.9 and the temperature ranges between 3.5 and 4.6°C (Fig. 5a, b). The variability in this temperature results from the absence or presence of flow of Alaskan Stream water through Amukta Pass. When flow is present, a signature of warm (>4.0°C) subsurface water is evident in the eastern basin and slope region (Reed 1995). Inferring lack of inflow from the absence of the warm subsurface water indicates that for periods of months inflow of Alaskan Stream water through Amukta Pass can be absent.

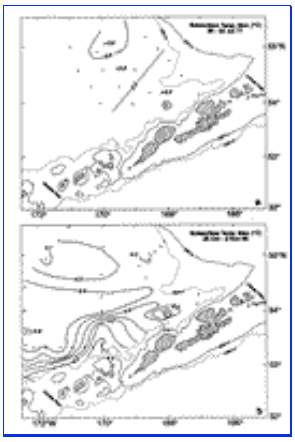

**Fig. 5. (a) Distribution of temperature (°C) at the subsurface maximum during a period when the temperature was at a minimum. (b) Distribution of the temperature of the subsurface maximum when substantial areas were >4.0°C. (This figure is adapted from Figs. 3 and 5 in Reed 1995).**

Few measurements have been made of transport through Amchitka Pass, the third deepest pass in the Aleutian Arc, and only three hydrocast sections have been reported in the literature through the narrow sill region at 51°28′N (Reed and Stabeno, chapter 8, this volume). Measured baroclinic transports range from 2.8 × $10^6$ $m^3$/s southward to 2.8 × $10^6$ $m^3$/s northward, with a mean of 0.3 × $10^6$ $m^3$/s northward. The flow pattern across the pass is similar to that observed through Amukta Pass, with inflow on the eastern side and outflow on the western side. The source of outflow is twofold. Some originates at Near Strait and Buldir

Pass and flows eastward across Bowers Ridge, while the remainder consists of a retroflection of the inflow through the eastern part of Amchitka Pass.

A vertical section of temperature and salinity reveals the inflow of Alaskan Stream water on the eastern side of the pass where the depth of the 4°C contour dipped to ~400 m (Fig. 6a). As suggested by isopleths, the net baroclinic transport was weak (0.3 × $10^6$ $m^3$/s northward). Two satellite-tracked drifters were deployed shortly after the CTD section in the vicinity of Amchitka Pass. The trajectories (Fig. 7) reveal the presence of two eddies that inhibited much of the flow through the pass. The northern drifter remained in the cyclonic eddy for 22 days, making 2.5 circuits around the northern eddy. The other drifter made four circuits of the southern eddy before malfunctioning. Typical speeds of rotation were the same for each eddy, 30 cm/s. Flow of significant amounts of Alaskan Stream water was thus blocked from the pass. During 1991, there was also evidence from drifter trajectories (not shown) of an eddy in the eastern portion of the pass, but these drifters did not remain in the eddy for more than one rotation. Evidence of an eddy in the Alaskan Stream south of Amchitka Pass which affected the transport through Amchitka Pass, was revealed in altimeter data (Okkonen 1996).

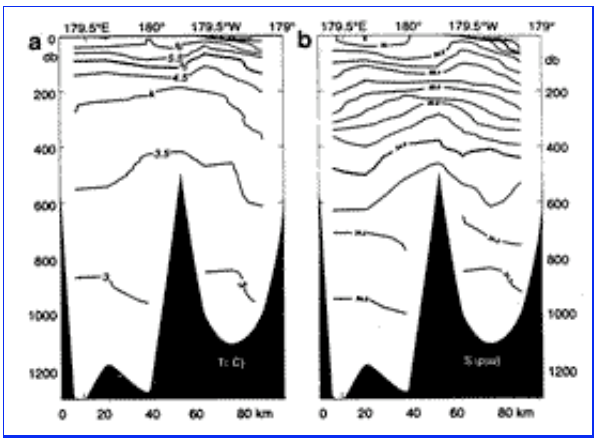


**Fig 6. Vertical sections of (a) temperature (°C) and (b) salinity (psu) along 51°30′N in Amchitka Pass on September 15, 1992.**

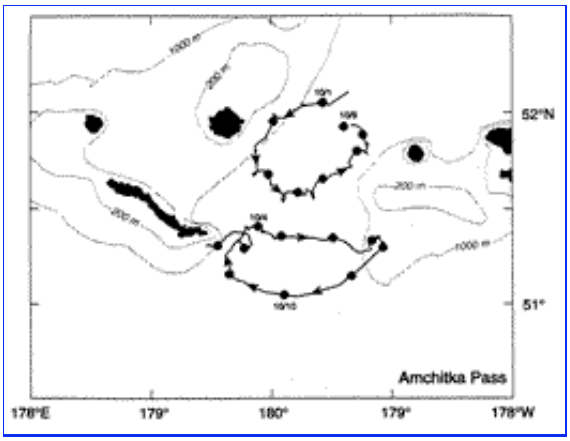


**Fig. 7. Trajectories from satellite-tracked drifting buoys deployed in the vicinity of Amchitka Pass in September 1992. Each drifter had a holey sock drogue at 40 m depth. Daily positions are indicated by circles on the trajectories. The southern drifter remained in the eddy for 25 days, making 2.5 circuits. The northern drifter made four circuits of the eddy. Mean rotational speed was 30 cm/s in both**

**eddies.**

Results from the one current meter mooring, which was positioned north of the pass, have been reported in the literature (Reed 1990). The net flow (14 cm/s) is to the northeast (Fig. 8). Interpretation of measurements from a single mooring within a bi-directional flow is ambiguous; however, results from this current meter integrated with hydrographic surveys suggest a northward flow of 2–3 × $10^6$ $m^3/s$ through the eastern part of the pass. Through the western portion of the pass a southward flow occurs, resulting in a net transport of probably 1–2 × $10^6$ $m^3/s$.

Virtually no direct measurements of current have been made in Buldir Pass. Trajectories of satellite-tracked drifters indicate that northward flow can occur through the pass. Stabeno and Reed (1992) estimated an inflow of less than 1.0 × $10^6$ $m^3/s$.

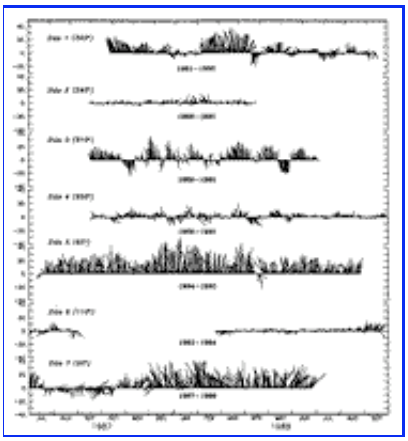

**Fig. 8. Daily currents measured at seven locations indicated in Fig. 2. A low pass filter (35-hour Lancoz squared) was applied to each series and the series were then rotated to their net direction (indicated in parentheses). The depth of each instrument was between 250 and 350 m. Site locations are shown in Fig. 1.**

Most of the transport into the Bering Sea occurs through Near Strait (6–12 × $10^6$ $m^3/s$). Historically, transport of Alaskan Stream water through Near Strait was estimated at ~10 × $10^6$ $m^3/s$ and believed to be relatively constant (Favorite 1974). More recent research indicates that the flow through this pass, as through the other passes, is extremely variable. Occasionally, instabilities (eddies) occur in the Alaskan Stream that inhibit flow into the Bering Sea through Near Strait. Such an eddy in 1991 resulted in a net northward baroclinic transport of less than 3 × $10^6$ $m^3/s$ (Stabeno and Reed 1992). Near Strait is the only deep pass that has been monitored with current moorings (Reed and Stabeno 1993). A series of moorings deployed in the eastern portion of the pass indicate that the periods of reduced inflow vary on scales of months. Yearly average velocity at ~100 m was 6 cm/s into the Bering Sea in the eastern portion of the pass, and decreased to 1–2 cm/s in the central part of the pass. It was moderately surprising that the strongest, steadiest flow occurred near the bottom of the narrow passage on the eastern side of the pass, a result of tidal rectification.

Not only is Kamchatka Strait the location of the majority of outflow, but it is the only conduit into the Bering Sea that is deep enough (>2,000 m) to permit inflow of Deep Pacific Water (DPW). In the upper 1500 m, flow is dominated by the southward-flowing Kamchatka Current on the western side of the strait and a weak inflow occurs on the eastern side (Stabeno and Reed 1994, Cokelet et al. 1996). The inflow of DPW occurs below 2,000 m predominately on the eastern side of the strait (Reed et al. 1993), and thus the

highest salinities in the Bering Sea basin are observed here (Fig. 9b). Salinities decrease in the basin as the high salinity DPW mixes with surrounding water. The Bering Sea deep water contains the highest concentrations of silica in the world's ocean (Mantyla and Reid 1983). Between 2,000 and 3,000 m, high concentrations of silica (>225 m M/L; Fig. 9c) occur in the strait (Reed et al. 1993). Concentrations similar to these are observed in the Bering Sea basin further to the northeast. This suggests a southward flow of deep Bering Sea water beneath the Kamchatka Current and above the inflow of DPW. Measurements of transport of the Kamchatka Current in the pass range from $5 \times 10^6$ m$^3$/s (Verkhunov and Tkachenko 1992) to $15 \times 10^6$ m$^3$/s (Ohtani 1970).

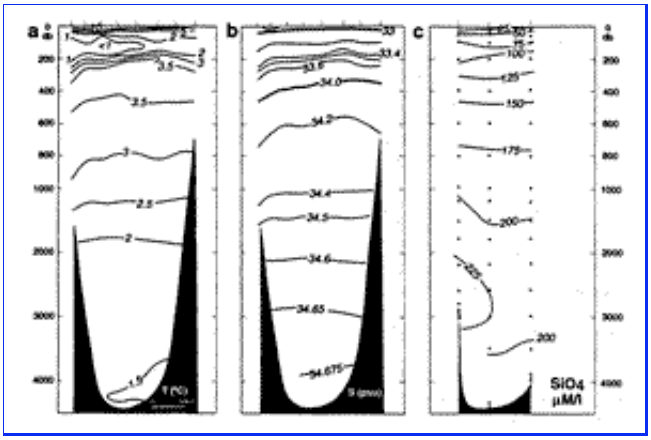


**Fig. 9. Vertical sections of (a) temperature, (b) salinity, and (c) silica (mM/L) across Kamchatka Strait on August 13–14 , 1991. Modified from Reed et al. (1993).**

## Mean Upper Ocean Circulation

General circulation over the deep basin is characterized by a cyclonic gyre, with three well-defined, distinct currents: the Kamchatka Current along the western boundary; the Bering Slope Current along the eastern boundary; and the Aleutian North Slope Current connecting the inflow through Amukta Pass and Amchitka Pass with the Bering Slope Current (Fig. 2). Transport within the gyre can vary by more than 50%. Modeling studies have simulated such large changes in transport and identified the causal mechanisms to be fluctuations of Alaskan Stream inflow (Overland et al. 1994) and/or changes in the wind-driven transport within the basin (Bond et al. 1994).

The main features of the upper-ocean circulation are shown in Fig. 3. This figure has been modified from those in Stabeno and Reed (1992, 1994) and Reed (1995). Much of the information is from the water property and geostrophic flow results from Favorite (1974), Hughes et al. (1974), and Sayles et al. (1979). Information from satellite-tracked drifting buoys is taken from Stabeno and Reed (1994) and from the limited number of current meter moorings which have been deployed in the basin. A more detailed flow field (Fig. 10) derived from satellite-tracked drifters (following Stabeno and Reed 1994) from 1984 through 1996, reveal each of the main current systems along with flow through the passes and weak westward flow across the basin.

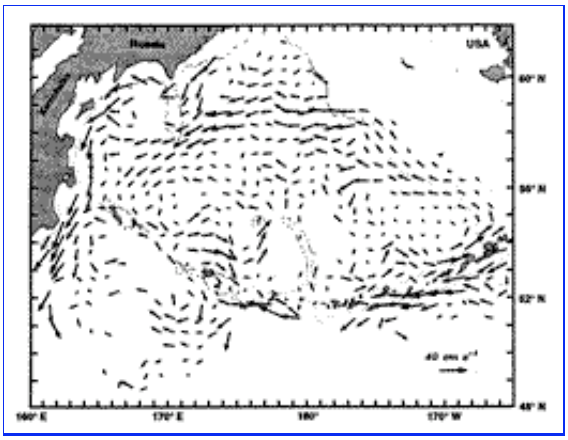

**Fig. 10. Velocity at 40 m derived from satellite-tracked drifters. The method used was the same as described in Stabeno and Reed (1994).**

### The Alaskan Stream

While the Alaskan Stream (AS) is not in the Bering Sea, it is the main source water for much of the flow that occurs in the Bering Sea and so merits a brief discussion. The AS, which is the northern boundary current of the Pacific subarctic gyre, extends from the head of the Gulf of Alaska to the western Aleutians. It is characterized as a narrow, high speed current, with small eddy kinetic energy to mean kinetic energy ($KE'/KE < 1.0$) from 165°W to 173°E (Stabeno and Reed 1990). It turns northwestward at Amchitka Pass (180°) following the bathymetry, slowing and broadening. Maximum daily averaged buoy speeds east of 180° were 70–95 cm/s, while to the west of 180° maximum speeds were 40–65 cm/s. Although the position of the Alaskan Stream relative to the Aleutian Islands is relatively constant, there is some variability, which, coupled with eddies, results in changes in transport through the passes.

### Aleutian North Slope Current

Although there is some indication of an eastward flow along the north side of the Aleutian Islands between Kamchatka Strait and Near Strait, and also between Near Strait and Amchitka Pass (Stabeno and Reed 1994), the only well-documented persistent eastward flow occurs east of Amchitka Pass (Reed and Stabeno, chapter 8, this volume). This current is strongly influenced by flow through the passes. East of Amchitka Pass, it is not completely continuous, but rather originates from inflow on the eastern side of one deep pass and continues eastward until it (or some portion) exits through the western side of the next deep pass.

The Aleutian North Slope Current (ANSC) is best documented between 174°W and 167°W by hydrographic surveys (Reed and Stabeno 1997), satellite-tracked drifting buoys (Stabeno and Reed 1994), and more recently in current meter records (Reed and Stabeno 1997). It is here that the flow merits being called a current. The ANSC is a narrow (~20 km), stable current that appears to have an annual signal, as indicated by both the trajectories of satellite-tracked drifting buoys and time series from current meter moorings. Currents (measured at mooring site 5, Fig. 1) are northeastward following bathymetry. Few reversals are evident in these 13-month-long current records (Fig. 8). The strongest daily average currents (>40 cm/s at 100 m) occur during winter, while the mean velocity at 100 m exceeds 20 cm/s. The flow at 50 m above the bottom has no seasonal signal and is statistically significant at 4.5 cm/s northeastward. The $KE'/KE$ ratio are very small (<0.5) in the upper ~300 m and near the bottom. This vertical structure, with decreasing speeds,

is also evident in baroclinic estimates of flow from hydrographic surveys. Measurements of baroclinic transport range from $3 \times 10^6$ m$^3$/s (Reed and Stabeno, chapter 8, this volume) to $5.5 \times 10^6$ m$^3$/s (unpublished data from February 1997).

**Bering Slope Current**

Eastward of 167°N, the ANSC turns northwestward, forming the Bering Slope Current (BSC), the eastern boundary current of the Bering Sea gyre (Schumacher and Reed 1992, Kinder et al. 1975). The characteristics of this flow differ markedly from the ANSC. This can easily be seen in comparing time series and statistics of two moorings, one in the ANSC and the other in the BSC (Fig. 1). Unlike the ANSC, the presence of an annual cycle is not clearly evident in the time series at any of the sites in the BSC (sites 1, 2, 3, and 4), although model simulations show an intensification in fall-winter (Overland et al. 1994). The reversals evident in the BSC time series are likely a result of eddies. Only weak flow occurs at the sites associated with the canyons (sites 2 and 4). At the northernmost site, the strong currents are associated with eddies and the background flow is weak. The eddy:mean kinetic energy ratios at site 3 best represent the BSC. Seaward of the 1000-m isobath the flow is more variable and the BSC is often less well defined. The mean velocity (site 3) at 100 m (11 cm/s) is approximately half that observed in the ANSC. The BSC is also shallower than the ANSC, with mean flow at 500 m ~1 cm/s. Total transport ($3–6 \times 10^6$ m$^3$/s) is of course similar to that observed in the ANSC. These are consistent with the BSC being wider than the ANSC.

The BSC is strongest and most persistent south of 56.5°N. Most of the flow separates from the slope at the latitude of Pribilof Canyon or Zymchug Canyon, forming the source of the weak westward flow across the basin (Stabeno and Reed 1994). To the north of 58°N the flow is still generally northwestward, but is weaker, more intermittent, and confined to shallower water depth.

Studies of the BSC suggest that two significantly different structures or modes exist. Many CTD surveys reveal an ill-defined, highly variable flow interspersed with eddies, meanders, and instabilities (Kinder et al. 1975, Reed 1991). Other surveys, however, have revealed a more regular northwestward flowing current (Reed and Stabeno 1989). The trajectories from the more than 50 satellite-tracked drifters deployed in the southeast Bering Sea support this dichotomy in the structure of the BSC. They reveal the strong variability in the flow patterns that occur along the shelf break. In some trajectories, the BSC appears as a well-behaved current flowing northwestward along the shelf break (Stabeno and Reed 1994). At other times, chaos dominates the dynamics of the system (Reed and Stabeno 1990). At still other times, eddies, ranging in size from ~40 km to 150 km, are imbedded in the flow (Schumacher and Stabeno 1994). The structure of the BSC directly influences both the advection and dynamics along the slope, and also the occurrence of across-shelf fluxes. This dichotomy of structure, of either a series of eddies or a uniform flow, is supported by numerical model simulations of the subarctic North Pacific portion of the NRL Pacific Ocean model.

**The Kamchatka Current**

The third distinct current system, the Kamchatka Current, forms the western boundary current of the Bering Sea gyre. It originates near 175°E (Shirshov Ridge), as the weak westward flow (Stabeno et al. 1994). The source of this water is a combination westward flowing water (from the BSC) and northward flowing water entering the Bering Sea through Near Strait (Stabeno and Reed 1994, Khen 1989). The bathymetric feature of Shirshov Ridge causes a southward deflection and reduction in speed of the current (Stabeno and Reed, 1994). As the Kamchatka Current continues southward along the Russian coast it both strengthens and deepens. Near Shirshov Ridge flow (>5 cm/s) is evident only in the upper 1,000 m, while in Kamchatka

Strait it has deepened to >1,500 m. The maximum daily averaged speeds observed in the Bering Sea occur in the Kamchatka Current (40–77 cm/s). Daily averaged velocities as large as 100 cm/s occur in Kamchatka Strait. Meanders and eddies are common in the Kamchatka Current (Solomon and Ahlnas 1978, Stabeno et al. 1994, Cokelet et al. 1996). These features cause the long-term mean velocities to be much smaller than observed in the more stable Alaskan Stream.

Favorite (1974) estimated the transport in the Kamchatka Current as ~10 × $10^6$ $m^3$/s, but recent results indicate that it can be quite variable ranging from 7 to 15 × $10^6$ $m^3$/s (Stabeno and Reed 1992, Reed and Stabeno 1993, Overland et al. 1994, Cokelet et al. 1996). Variations in wind-stress curl are substantial with a winter maximum and might affect the transport (Overland et al. 1994, Bond et al. 1994). At times flow in the Kamchatka Current recirculates in the Bering Sea, with only a portion flowing through Kamchatka Strait and the remainder flowing eastward along the north side of the Aleutian Island (Reed et al. 1993).

## Interior Flow

Resulting from the strong inflow through Near Strait, a weak northward flow is evident in buoy trajectories and model results over the basin (Figs. 2 and 10). The BSC is the source of the westward flow across the basin (Royer and Emery 1984), which originated at the two areas along the slope where the 1,000-m isobath is oriented east-west (Stabeno and Reed 1994). At the southern source (~56.5°N) the flow bifurcates with a significant portion forming a small sub-gyre in the southeast corner of the basin. At the northern source (~58°N) the flow continues eastward across the center of the basin.

There have been no long-term current moorings in the central basin, but a mooring (site 6) has been located in the southeast Bering Sea (2,200 m water depth) during spring and summer of 1992–1994 (Fig. 8). These records show generally weak flow interrupted by eddies (Cokelet and Stabeno 1997). The background flow contrasts sharply from the other two sites (one in the ANSC and the other in the BSC) discussed earlier. At 80 m the flow is weakly northward (~1 cm/s) with high eddy-mean kinetic energy ratios. Below 150 m the currents are negligible. The eddies that intersperse the weak background flow are far more energetic.

## Eddies

As elsewhere in the world's oceans, eddies are ubiquitous in the Bering Sea (Solomon and Ahlnas 1978, Kinder et al. 1980, Paluszkiewcz and Niebauer 1984, Schumacher and Stabeno 1994). They occur on horizontal scales ranging from ~10 km to 200 km. Proposed mechanisms for the creation of these eddies include instabilities, wind forcing, strong flows through the eastern passes, and topographic interactions (Schumacher and Stabeno 1994).

The influence of eddies in straits have already been discussed, as has the presence of eddies in the BSC. One of the best time series, showing eddies in the basin has been collected during the spring and summer over a 3-year period at site 6. Eddies are common in these current records. These observations characterize the eddies as often anti-cyclonic, 20–100 km in diameter, extending to a depth of 400–1000 m, and with rotational speeds >20 cm/s (Schumacher and Stabeno 1994, Cokelet and Stabeno 1997).

On the western side of the basin, eddies result from instabilities in the Kamchatka Current. The eddies are often anti-cyclonic, 20–100 km in diameter, and have rotational speeds of >40 cm/s. They have been observed in satellite-tracked buoy trajectories, hydrographic surveys, and satellite images (Solomon and Ahlnas 1978). In three embayments on the Kamchatka Peninsula anti-cyclonic eddies were evident in the

tracks of many of the buoys. They resulted from the interaction of the Kamchatka Current with topographic features and are likely semi-permanent, since they appeared in trajectories from more than 1 year (Schumacher and Stabeno 1998).

West of Bowers Ridge a large (~200 km), energetic (velocities ~30–40 cm/s) eddy was observed in 1991 (Reed et al. 1993, Cokelet et al. 1996). Buoys were deflected around the feature, with none entrained into the center. Although this feature persisted for several months, it was only observed during 1991. Thus its persistence is unknown.

Eddies are common at the eastern shelf break and shoreward to depths of ~150 m. A recent interpretation of hydrographic observations (Reed, in press) suggests anticyclonic eddies exist in the region between 100 and 122 m <20% of the time. Shoaler than 100 m, eddies are uncommon.

## Deep Circulation

Little comprehensive information is available on deep circulation in the Bering Sea. However, a study that examines all of the available information on deepwater properties, and infers flow, is nearing completion (T. E. Whitledge, University of Texas at Austin, pers. comm., November 1995 [now at University of Alaska Fairbanks, School of Fisheries and Ocean Sciences, Fairbanks, AK 99775-7220]). Sayles et al. (1979) presented limited data to 2,500 m and inferred flow at 1,000 and 1,400 m, referred to 2,500 m. The only significant flow at these levels was the Kamchatka Current.

Reed et al. (1993) presented vertical sections of temperature salinity sigma-*t*, and silica across the Kamchatka Strait. Inflow of deep water occurred below 2,500 m on the eastern side of the strait. Silica data suggested a return flow of upper deep water (near 2,500 m) on the western side of the strait. In July 1993, a World Ocean Circulation Experiment section was occupied in the Bering Sea from the continental slope southwestward through Amchitka Pass (Roden 1995). The deep Bering Sea is warmer, less salty, less dense, less oxygenated, and with greater concentrations of silica than the open waters south of the Aleutians. Silica increases somewhat near the continental slope (Roden 1995, Tsugonai et al. 1979). Clearly more data are needed, but the path of deep water must be northward and eastward from Kamchatka Strait with some return flow above 3,000 m on the western side of the strait. The map of deep flow is consistent with hydrographic data and water properties (Fig. 11).

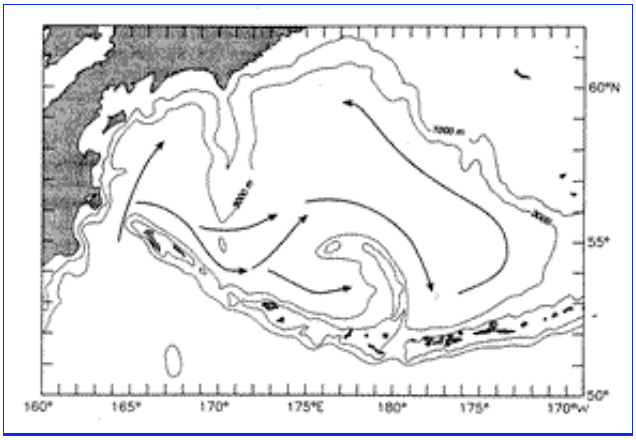


**Fig. 11. The deep flow in the Bering Sea basin below 3,000 m. This pattern is inferred from water properties as described in the text.**

We are not aware of any long-term measurements of flow below 1,000 m. A year-long record at ~1,000 m depth along the eastern shelf break indicates that all significant flow occurred above 500 m (Schumacher and Reed 1992). Reed (1995) reviewed previous efforts to establish reference levels for geostrophic flow computations in the western Bering Sea near the Kamchatka Current. Deep levels (to 3,000 m) appeared most suitable, but levels of 1,500 m or above were suggested for the eastern Bering Sea. Cokelet et al. (1996), compared measurements between an acoustic Doppler current profiler and geostrophic shear; these results supported the regional pattern suggested above.

## Shelf-Slope Exchange

A connection exists between the basin and shelf that is fed by shelf-slope exchange. The northward transport through Bering Strait ($0.8 \times 10^6$ m$^3$/s) and through Unimak Pass requires a net onshelf transport of ~$0.5 \times 10^6$ m$^3$/s. One school of thought is that a "river" of water flows onto the northern shelf. This is manifest in some schematics (e.g., Shuert and Walsh 1993) that show the BSC flowing northward along the slope and bifurcating south of Cape Navarin. One branch (sometimes called the Anadyr Current) then flows across isobaths along the Gulf of Anadyr where a canyon exists which influences model simulations (e.g., Overland and Roach 1987) through Anadyr Strait and thence to Bering Strait. Direct observations (Stabeno and Reed 1994), however, show that the BSC tends to leave the slope near 59°N and then flow eastward. While temperature, salinity, and nutrient concentrations in the waters that eventually go through Bering Strait are all of slope origin, their source is likely not a "river" which flows from the basin onto the shelf south of Cape Navarin (Schumacher and Stabeno 1998).

Shelf-slope exchange can occur virtually anywhere along >1,200 km of shelfbreak north of Unimak Pass. Two regions exist where preferential transport onto the shelf has been observed. The first is Bering Canyon which lies along the Aleutian Islands near Unimak Pass. The enhanced concentration of nutrients observed near Unimak Pass likely originate from ANSC waters interacting with canyon topography and coming onto the shelf (Schumacher and Stabeno 1998). The second region occurs west of Pribilof Islands, where the narrowing of the shelf break accelerates the flow along the 100-m isobath, which then turns northward. The accelerated flow over the outer shelf between St. George Island and Pribilof Canyon results in water being entrained from the adjacent slope (Salo et al., chapter 9, this volume). Flow near the Pribilof Islands is evident in satellite-tracked drifter trajectories (drogue depth 40 m).

Episodic events of onshelf flow have been observed resulting from both eddy-topography interactions and as a result of instabilities in the BSC (van Meurs and Stabeno, in press). Along the slope of the central shelf (~56.7°N), current records reveal that eddies are common and estimates of salt and temperature fluxes indicate that significant onshore fluxes exists (Schumacher and Reed 1992). In 1992 an excellent set of data was collected when an eddy translated onto the shelf (Schumacher and Stabeno 1994). Three satellite-tracked drifters had been deployed in the center of an eddy. The drifters remained in the eddy for weeks, until the eddy moved eastward onto the shelf. The drifters were deposited onto the shelf as the eddy spun down. Both of these episodic events of onshelf flow were related to the stability of the BSC.

The net effect of onshelf fluxes from the slope, either regionally or by intermittent processes, is the presence of slope waters over the outer shelf of the eastern Bering Sea. Using the generally accepted value of mean speed along both the southeastern and central outer shelf (0.05 m/s in the upper 100 m of the ~100 km wide domain), we compute a transport of $0.5 \times 10^6$ m$^3$/s. It is these waters that are westward intensified and become the strong steady current that flows through Anadyr Strait, providing nutrients for the high productivity observed there.

# Shelf Flow

## Low Frequency Currents

The schematic of flow on the eastern shelf (Fig. 2) is a synthesis of moorings, satellite-tracked drifting buoys, and hydrographic sections (Schumacher and Stabeno 1998). Flow through Unimak Pass results in a weak, although persistent, flow along the 50-m isobath. Measurements are not sufficient to determine if there is a seasonal signal in this flow, reflecting the variability of the flow through Unimak Pass. The flow along 50-m isobath continues through Shpanberg Pass and accounts for about a third of the flow through Bering Strait (0.35 $m^3/s$). Some flow through Unimak Pass follows along the 100-m isobath (Reed and Stabeno, submitted). This flow continues northwestward along the ~100 m isobath, although its position appears to vary on annual or longer scales (Reed, in press). It is augmented by the onshelf flow associated with Bering Canyon and episodic events. Additional flux of onshelf flow occurs south of the Priblof Islands. North of the Pribilof Islands a portion of northward flow along the 100 m isobath separates and flows eastward across the shelf, augmenting the flow through Unimak Pass. The flow that continues along the 100-m isobath appears as a broad, slow northwestward flow.

This northward flow intensifies along the east coast of Siberia forming the only strong low-frequency currents on the shelf (the Anadyr Current). The flow turns eastward across the shelf along the southern coast of Siberia and eventually exits the Bering Sea through Bering Strait. The flow through Bering Strait dominates the current dynamics of the northern shelf.

The freezing and melting of sea ice can result in a distribution of mass that generates baroclinic flow. As with all high latitude seas, sea ice is one of the primary characteristics of the Bering Sea. For approximately half the year the Bering Sea is free of ice, but during November ice begins to form or be advected into the Bering Sea through Bering Strait. Although the ice is generally limited to the Bering Sea shelves, the extent of the seasonal advance is the largest observed in any arctic or subarctic region. The formation of the ice is best described by "conveyor belt" analogy (Pease 1980, Overland and Pease 1982). Ice forms along the leeward side of the coasts and islands in polynyas (open regions of water). The ice is then advected southward (or southwestward) where it is melted by the warmer water. At the polynyas the freezing sea water produces regions of high salinity (>34 psu) and at the melting edge the ice freshens the water (~30 psu). The amount of production and advection of ice depends upon which storm track dominates in a given winter, with greatest ice production occurring in years when the Aleutian Low is well developed and storms migrate along the primary storm track. By late March or April, the ice generally has begun to retreat, leaving behind a freshened water column and shelf with relatively cold water.

Cold saline water from the Gulf of Anadyr and Anadyr Strait polynyas provides a substantial fraction of the total salt advected into the Arctic Ocean (Cavalieri and Martin 1994). The ice melt produces a lens of fresh water that can assist in the formation of a strong two-layer system over the middle Bering Sea shelf. Associated with ice melt is a bloom of phytoplankton (during April) that accounts for 10–65% of the total annual primary production over the eastern shelf (Niebauer et al. 1990, Stabeno et al. 1998) with estimates of 45–70% for the western shelf (Mordasova 1995). During years when the ice is not present over the southeastern Bering Sea shelf, the spring bloom is delayed (May).

Far less is known about the flow along the western shelf. Satellite-tracked drifter trajectories reveal a narrow, westward flowing current (15–25 cm/s) along the south coast of Siberia. These observations support the inferred flow from water property distributions.

### Tidal Currents

Tides enter the Bering Sea from the Pacific Ocean, and to a much lesser degree from the Arctic Ocean through Bering Strait (Pearson et al. 1981, Mofjeld 1986). Most of the kinetic energy south of 60°N is provided by tidal currents. North of this latitude the strength of the tides decreases and the mean flow strengthens (Schumacher and Stabeno 1998, Coachman 1986).

Tidal currents play a vital role in the physical oceanography over the shelves. They provide sufficient energy to mix the bottom ~40 m of water over the southeastern shelf, thus setting up a two-layer density structure in water depths of 50–100 m. Shoaler than this the water column is weakly stratified or well mixed (Schumacher and Stabeno 1998). Tidal currents may contribute to the cross-shelf flux of salt, nutrients and heat necessary to maintain the high levels of primary production over the eastern shelf. Tidal currents also provide a mechanism for the generation of subtidal flow resulting from rectification of tidal currents with topography (Kowalik, chapter 4, this volume).

## Future Directions

While our knowledge of the physical oceanography of the Bering Sea has expanded greatly over the past few decades, many phenomena exist which are not understood primarily because observations are limited or do not exist. That a vast percentage of the Bering Sea lies within the domain of two different nations has not facilitated research programs that could provide the needed observations. Further, while the eastern continental shelf continues to have ongoing research programs and interest in the role of physical processes over the western shelf is growing, the deep basin remains largely unexamined.

The Bering Sea is a vital part of the general circulation of the North Pacific Ocean; fluxes of heat, salt, nutrients, and other dissolved constituents and planktonic material are exchanged through the passes. Primary questions, however, remain about the variability, magnitude and mechanisms influencing transport through the Aleutian Passes. In contrast, the flux northward through Bering Strait, which is important to conditions on the Arctic shelves and ocean, is relatively well described and understood.

While it is recognized that flow through the passes is a primary source of circulation within the basin, many questions remain regarding the current systems of the Bering Sea. What is the nature of the annual signal of the ANSC, and if there is a significant annual signal, does it occur in both speed and transport? The BSC apparently can be characterized by two modes, yet the phenomena that generate these are not known. While some studies have elucidated the nature of the Kamchatka Current, little is know of the temporal variability in transport and eddy kinetic energy. What is the magnitude and variability of inflow of DPW into the Bering Sea Basin? The flow patterns of the deep basin have been inferred from a limited number of hydrocasts, so we know neither the temporal nor spatial variability. The behavior of the source waters for deep circulation, the inflow of the DPW through Kamchatka Pass, is not known.

The processes that result in the exchange of slope and shelf waters have not yet been determined. Hence, we do not know the mechanisms that provide nutrients to the euphotic zone and are responsible for the region of prolonged biological production known as the "Green Belt" (Springer et al. 1996). While the processes are unknown, the results of their interactions are evident. The continental shelf of the Bering Sea exhibits extremely high productivity, and this richness applies throughout the food chain. Not only are there vast quantities of commercially valuable species, but the eastern shelf is the summer feeding ground for

numerous marine bird and marine mammal populations of the North Pacific Ocean. The eastern Bering Sea provides an ideal location to examine exchange mechanisms between slope water of an eastern boundary current and a continental shelf. Because the coast and its inherent topographic and coastal convergence processes are far removed from the slope, the processes involved in shelf/slope exchange should provide a clear signal. The continental shelf of the western Bering Sea is bounded by a typical western boundary current, so that contrasts of processes between the eastern and western shelves should be fruitful.

Future studies that focus on how the extant physical phenomena affect marine populations offer the best opportunity to enhance our understanding of ecosystem dynamics. This, in turn, could lead to management strategies aimed at sustainable production to ensure a rich ecosystem for our future generations. The observational database for the Bering Sea is not adequate, in both spatial and temporal coverage, to answer most of the questions noted above. In addition to further observations, modeling efforts need to be improved. A primitive equation basin-shelf model coupled to both outflow through Bering Strait and exchange in the North Pacific Ocean is a likely starting place. Once the model provides accurate simulations of the physical features, then biophysical processes and rates can be incorporated. Some of the questions that must be addressed to understand the ecosystem are best investigated by modeling efforts.

# Acknowledgments

We thank the numerous scientists who planned, conducted, and published their research. We also thank all the technical staff who assisted with the data acquisition, preparation, and analysis. This contribution was funded by the Coastal Ocean Programs Bering Sea FOCI and by the Fisheries Oceanography Coordinated Investigations of NOAA (#BS302), and is Pacific Marine Environmental Laboratory's contribution #1878.

# References

Aagaard, K., L.K. Coachman, and E. Carmack. 1985a. On the halocline of the Arctic Ocean. Journal of Geophysical Research 90:4833–4846.

Aagaard, K., J.D. Schumacher, and A.T. Roach. 1985b. On the wind-driven flow through Bering Strait. Journal of Geophysical Research 90:7213–7221.

Arzhanova, N.V., V.L. Zubarevich, and V.V. Sapozhnikov. 1995. Seasonal variability of nutrient stocks in the euphotic zone and assessment of primary production in the Bering Sea. In: B.N. Kotenev and V.V. Sapozhnikov (eds.), Complex studies of the Bering Sea ecosystem, VNIRO, Moscow, pp. 162–179.

Bond, N.A, J.E. Overland, and P. Turet. 1994. Spatial and temporal characteristics of the wind forcing of the Bering Sea. Journal of Climate 7:1119–1130.

Bryan, K., and M.J. Spelman. 1985. The ocean's response to a $CO_2$-induced warming. Journal of Geophysical Research 90:11,679–11,688.

Cavalieri, D.J., and S. Martin. 1994. The contribution of Alaskan, Siberian, and Canadian coastal polynyas to the cold halocline layer of the Arctic Ocean. Journal of Geophysical Research 99:18,343–18,362.

Coachman, L.K. 1986. Circulation, water masses, and fluxes on the southeastern Bering Sea shelf. Continental Shelf Research 5:23–108.

Coachman, L.K. 1993. On the flow field in the Chirikov Basin. Continental Shelf Research 13:481–508.

Coachman, L.K., K. Aagaard, and R.B. Tripp. 1975. Bering Strait: The regional physical oceanography. University of Washington Press, Seattle, 172 pp.

Cokelet, E.D., and P.J. Stabeno. 1997. Mooring observations of the thermal structure, density stratification and currents in the southeast Bering Sea basin. Journal of Geophysical Research 102(C10):22,947–22,964.

Cokelet, E.D., M.L. Schall, and D. Dougherty. 1996. ADCP-referenced geostrophic circulation in the Bering Sea basin. Journal of Physical Oceanography 26:1113–1128.

Favorite, F. 1974. Flow into the Bering Sea through Aleutian island passes. In: D.W. Hood and E.J. Kelley (eds.), Oceanography of the Bering Sea with emphasis on renewable resources, Occasional Publication No. 2, Institute of Marine Science, University of Alaska, Fairbanks, pp. 3–37.

Hughes, F.W., L.K. Coachman, and K. Aagaard. 1974. Circulation, transport and water exchange in the western Bering Sea. In: D.W. Hood and E.J. Kelley (eds.), Oceanography of the Bering Sea with emphasis on renewable resources, Occasional Publication No. 2, Institute of Marine Science, University of Alaska, Fairbanks, pp. 59–98.

Khen, G.V. 1989. Oceanological conditions of the Bering Sea biological productivity. In: Proceedings of the International Scientific Symposium on Bering Sea Fisheries, NOAA Tech. Memo NMFS F/NWC-163, pp. 404–414. (Available through NTIS.).

Kinder, T.H., L.K. Coachman, and J.A. Galt. 1975. The Bering Slope Current System. Journal of Physical Oceanography 5:231–244.

Kinder, T.H., J.D. Schumacher, and D.V. Hansen. 1980. Observations of a baroclinic eddy: An example of mesoscale variability in the Bering Sea. Journal of Physical Oceanography 10:1228–1245.

Mantyla, A.W., and J.L. Reid. 1983. Abyssal characteristics of the world ocean waters. Deep-Sea Research 30:805–833.

Mofjeld, H.O. 1986. Observed tides on the Northeastern Bering Sea Shelf. Journal of Geophysical Research 91:2593–2606.

Mordasova, N.V. 1995. Chlorophyll in the western Bering Sea. Oceanology 34:503–509. (English translation.)

Niebauer, H.J. 1988. Effects of El Niño-Southern Oscillation and North Pacific weather patterns on interannual variability in the subarctic Bering Sea. Journal of Geophysical Research 93:5051–5068.

Niebauer, H.J., and R.H. Day. 1989. Causes of interannual variability in the sea ice cover of the eastern Bering Sea. Geology Journal 18:45–59.

Niebauer, H.J., V. Alexander, and S. Henrichs. 1990. Physical and biological oceanographic interaction in the spring bloom at the Bering Sea marginal ice edge zone. Journal of Geophysical Research 95:22,229–22,242.

Niebauer, H.J., V. Alexander, and S.M. Henrichs, 1995. A time-series study of the spring bloom at the Bering Sea ice edge. I: Physical processes, chlorophyll and nutrient chemistry. Continental Shelf Research 15:1859–1878.

Nihoul, J.C.J., P. Adam, P. Brasseur, E. Deleersnijder, S. Djenidi, and J. Haus. 1993. Three-dimensional general circulation model of the Northern Bering Sea's summer ecohydrodynamics. Continental Shelf Research 13:509–542.

Ohtani, K. 1970. Relative transport in the Alaskan Stream in winter. Journal of the Oceanographic Society of Japan 26:271–282.

Okkonen, S.R. 1996. The influence of an Alaskan Stream eddy on flow through Amchitka Pass. Journal of Geophysical Research 101:8839–8852.

Overland, J.E. 1981. Marine climatology of the Bering Sea. In: D.W. Hood and J.A. Calder (eds.), The Eastern Bering Sea shelf: Oceanography and resources, volume one. Published by the Office of Marine Pollution Assessment, National Oceanic and Atmospheric Administration and Bureau of Land Management, pp. 15–30. (Distributed by the University of Washington Press, Seattle, WA 98105.)

Overland, J.E., and C.H. Pease. 1982. Cyclone climatology of the Bering Sea and its relation to sea ice extent. Monthly Weather Review 110:5–13.

Overland, J.E., and A.T. Roach. 1987. Northward flow in the Bering and Chukchi seas. Journal of Geophysical Research 92:7097–7105.

Overland, J.E., M.C. Spillane, H.E. Hurlburt, and A.J. Wallcraft. 1994. A numerical study of the circulation of the Bering Sea basin and exchange with the North Pacific Ocean. Journal of Physical Oceanography 24:736–758.

Paluszkieicz, T., and H.J. Niebauer. 1984. Satellite observations of circulation in the eastern Bering Sea. Journal of Geophysical Research 89:3663–3678.

Pearson, C.A., H.O. Mofjeld, and R.B. Tripp. 1981. Tides of the Eastern Bering Sea Shelf. In: D.W. Hood and J.A. Calder (eds.), The Eastern Bering Sea shelf: Oceanography and resources, volume two. Published by the Office of Marine Pollution Assessment, National Oceanic and Atmospheric Administration and Bureau of Land Management, pp. 111–130. (Distributed by the University of Washington Press, Seattle, WA 98105.)

Pease, C.H. 1980. Eastern Bering Sea ice processes. Monthly Weather Review 108:2015–2023.

Reed, R.K. 1990. A year-long observation of water exchange between the North Pacific and the Bering Sea. Limnology and Oceanography 35:1604–1609.

Reed, R.K. 1991. Circulation and water properties in the central Bering Sea during OCSEAP studies, Fall 1989–Fall 1990. NOAA Technical Report, ERL 446-PMEL 41, NTIS PB90-155847, 13 pp.

Reed, R.K. 1995. On the variable subsurface environment of fish stocks in the Bering Sea. Fisheries Oceanography 4:317–323.

Reed, R.K. In press. Confirmation of a convoluted flow over the southeastern Bering Sea shelf. Continental Shelf Research.

Reed, R.K., and P.J. Stabeno. 1989. Circulation and property distributions in the Central Bering Sea, Spring 1988. NOAA Technical Report, ERL 439-PMEL 39, NTIS PB90–155847, 13 pp.

Reed, R.K., and P.J. Stabeno. 1990. Flow trajectories in the Bering Sea: Evidence for chaos. Geophysical Research Letters 17:2141–2144.

Reed, R.K., and P.J. Stabeno. 1993. The return of the Alaskan Stream to Near Strait. Journal of Marine Research 51:515–527.

Reed, R.K., and P.J. Stabeno. 1994. Flow along and across the Aleutian Ridge. Journal of Marine Research 52:639–648.

Reed, R.K., and P.J. Stabeno. 1996. On the climatological net circulation over the eastern Bering Sea shelf. Continental Shelf Research 16(10):1297–1305.

Reed, R.K., and P.J. Stabeno. 1997. Long-term measurements of flow near the Aleutian Islands. Journal of Marine Research 55:565–575.

Reed, R.K., and P.J. Stabeno. Submitted. Inflow through Unimak Pass, Alaska. Geophysical Research Letters.

Reed, R.K., G.V. Khen, P.J. Stabeno, and A.V. Verkhunov. 1993. Water properties and flow over the deep Bering Sea basin, summer 1991. Deep-Sea Research 40:2325–2334.

Roach, A.T., K. Aagaard, C.H. Pease, S.A. Salo, T. Weingartner, V. Pavlov, and M. Kulakov. 1995. Direct measurements of transport and water properties through Bering Strait. Journal of Geophysical Research 100:18,443–18,457.

Roden, G.I. 1995. Aleutian Basin of the Bering Sea: Thermohaline, oxygen, nutrient and current structure in July 1993. Journal of Geophysical Research 100:13,539–13,554.

Royer, T.C., and W.I. Emery. 1984. Circulation in the Bering Sea, 1982–1983, based on satellite-tracked drifter observations. Journal of Physical Oceanography 14:1914–1920.

Sayles, M.A., K. Aagaard, and L.K. Coachman. 1979. *Oceanographic Atlas of the Bering Sea Basin*. University of Washington Press, Seattle, 158 pp.

Schumacher, J.D., and T.H. Kinder. 1983. Low-frequency current regimes over the Bering Sea shelf. Journal of Physical Oceanography 13:607–623.

Schumacher, J.D., and R.K. Reed. 1992. Characteristics of currents over the continental slope of the eastern Bering Sea. Journal of Geophysical Research 97:9423–9433.

Schumacher, J.D., and P.J. Stabeno. 1994. Ubiquitous eddies of the eastern Bering Sea and their coincidence with concentrations of larval pollock. Fisheries Oceanography 3:182–190.

Schumacher, J.D., and P.J. Stabeno. 1998. The continental shelf of the Bering Sea. In: A.R. Robinson and K.H. Brink (eds.), The Sea: The global coastal ocean regional studies and synthesis, Vol. XI. John Wiley and Sons, New York, pp. 869–909.

Schumacher, J.D., C.A. Pearson, and J.E. Overland. 1982. On exchange of water between the Gulf of Alaska and the Bering Sea through Unimak Pass. Journal of Geophysical Research 87:5785–5795.

Shuert, P.G., and J.J. Walsh. 1993. A coupled physical-biological model of the Bering-Chukchi seas. Continental Shelf Research 13:543–573.

Solomon, H., and K. Ahlnas. 1978. Eddies in the Kamchatka Current. Deep-Sea Research 25:403–410.

Springer, A.M., C.P. McRoy, and M.V. Flint. 1996. The Bering Sea Green Belt: Shelf edge processes and ecosystem production. Fisheries Oceanography 5:205–223.

Stabeno, P.J., and R.K. Reed. 1990. Recent Lagrangian measurements along the Alaskan Stream. Deep-Sea Research 38:289–296.

Stabeno, P.J., and R.K. Reed. 1992. A major circulation anomaly in the western Bering Sea. Geophysical Research Letters 19:1671–1674.

Stabeno, P.J., and R.K. Reed. 1994. Circulation in the Bering Sea basin by satellite tracked drifters. Journal of Physical Oceanography 24:848–854.

Stabeno, P.J., R.K. Reed, and J.E. Overland. 1994. Lagrangian measurements in the Kamchatka Current and Oyashio. Journal of Oceanography 50:653–662.

Stabeno, P.J., R.K. Reed, and J.D. Schumacher. 1995. The Alaska Coastal Current: Continuity of transport and forcing. Journal of Geophysical Research 100:2477–2485.

Stabeno, P.J., J.D. Schumacher, R.F. Davis, and J.M. Napp. 1998. Under-ice observations of water column temperature, salinity and spring phytoplankton dynamics: Eastern Bering Sea shelf. Journal of Marine Research 56:239–255.

Tsugonai, S., M. Kusakabe, H. Iizumi, I. Koike, and A. Hattori. 1979. Hydrographic features of the deep water of the Bering Sea, the sea of silica. Deep Sea Research, Part A 26:641–659.

van Meurs, P., and P.J. Stabeno. In press. Evidence of episodic on-shelf flow in the southeastern Bering Sea. Journal of Geophysical Research.

Verkhunov, A.V., and Y.Y. Tkachenko. 1992. Recent observations of variability in the Western Bering Sea Current system. Journal of Geophysical Research 97:14,369–14,378.

Walsh, J.J., C.P. McRoy, L.K. Coachman, J.J. Georing, J.J. Nihoul, T.E. Whitledge, T.H. Blackburn, P.L. Parker, C.D.Wirick, P.G. Shuert, J.M. Grebmeier, A.M. Springer, R.D. Tripp, D.A. Hansell, S. Djenidi, E. Deleersnijder, K. Henriksen, B.A. Lund, P. Andersen, F.E. Müller-Karger, and K. Dean. 1989. Carbon and nitrogen cycling with the Bering/Chukchi Seas: Source regions for organic matter affecting AOU demands of the Arctic Ocean. Progress in Oceanography 22:277–359.

Return to Abstract

Return to Outstanding Publications Page

Return to PMEL Publications Page

Return to PMEL Home Page

---